RESEARCH ARTICLE | DECEMBER 04 2020

Analysis of some structural, electronic and optical properties of Zn_nTe_n (n=1, 7, 11, 13) nanostructures: A DFT/TD-DFT study FREE

Hussein Hakim Abed ✉; Laith Taj-Aldeen; Mudar Ahmed Abdulsattar; Hayder M. Abduljalil; Ahmed Hashim; Saif M. Alghazaly

AIP Conf. Proc. 2290, 050043 (2020)
https://doi.org/10.1063/5.0028355

Analysis of Some Structural, Electronic and Optical Properties of Zn_nTe_n (n=1, 7, 11, 13) Nanostructures: A DFT/TD-DFT Study

Hussein Hakim Abed[1, a)], Laith Taj-Aldeen[1], Mudar Ahmed Abdulsattar[2, b)], Hayder M. Abduljalil[1, c)], Ahmed Hashim[3] and Saif M. Alghazaly[1]

[1] *Department of Physics, College of Science, University of Babylon, Iraq.*
[2]*Ministry of Science and Technology, Baghdad, Iraq.*
[3]*Department of Physics, College of Education of Pure Science, University of Babylon, Iraq*

[a)] Corresponding author: *hakimhussein.2017@gmail.com*
[b)]*mudarahmed3@yahoo.com*
[c)]*hayder_abduljalil@yahoo.com*

Abstract. Some of the structural properties, electronic properties and UV-Vis spectra of zinc telluride diamondoids nanostructures Zn_nTe_n (n=1, 7, 11, 13) have been investigated theoretically by using the Gaussian 09 package, density functional theory and time-dependent density functional theory at the B3LYP level with SDD (Stuttgart-Dresden pseudopotentials) basis function. The structural properties showed that the average Zn-Te bond length of all diamondoids converged to the experimental value 2.406Å and hexamantane $Zn_{13}Te_{13}$ has the longest bond length of 2.708 Å. Binding energy per atom indicated that the tetramantane $Zn_{11}Te_{11}$ more stable than other diamondoids because it has the largest binding energy of 2.352 eV/atom and the smallest ratio of dangling to total bonds. The energy gap decreased with increasing in diamondoids size and tend to touch the practical value 2.26 eV, hexamantane $Zn_{13}Te_{13}$ has an energy gap equal to 2.56 eV. UV-Vis spectra for tetramantane $Zn_{11}Te_{11}$ and hexamantane $Zn_{13}Te_{13}$ refer to redshift with an increased size of diamondoids. Tetramantane $Zn_{11}Te_{11}$ has a maximum peak at 345.6 nm and 410.4 nm for hexamantane $Zn_{13}Te_{13}$. These results refer to the ability to control the ZnTe properties by varied diamondoids sizes. These lead to wide applications in different fields such as optoelectronic devices, photoelectronic devices, detectors, and sensors.

Keywords: Zinc telluride, Diamondoids, DFT/TD-DFT.

INTRODUCTION

Nanostructures or Quantum Dots (QDs) of II-VI materials have interesting properties such as they have a wide energy gap, narrow photoluminescence, high stability, and size-dependent electronic, optical, and magnetic properties. Therefore, they are used in wide applications such as light-emitting diodes LEDs, biological photoelectrochemical cells, catalysts, solar cells and sensors [1-4]. Zinc Telluride (ZnTe), an II-VI semiconductor, has a direct bandgap of 2.26 eV at room temperature, large photoconductivity, and high excitonic binding energy. Therefore, it is an attractive material because of has several applications in optoelectronic and photo-electronic devices such as green light-emitting diodes, electro-optic field detectors, laser diodes, solar cells and sensors [5-8]. Fabrications semiconductors in the nano-scale regime have amazing progress in material science. In this regime, the quantum confinement and surface effect become predominant, causing many remarkable electronic and optical properties different from the bulk [9]. Hence, to study the materials at their nanoscale regime, a molecular species representing the seed (unit cell) are required to build the nanostructures.

The 8th International Conference on Applied Science and Technology (ICAST 2020)
AIP Conf. Proc. 2290, 050043-1–050043-8; https://doi.org/10.1063/5.0028355
Published by AIP Publishing. 978-0-7354-4020-3/$30.00

Bong H. B. and et al. calculated the structures and energies of low-lying isomers of ZnxSex (x = 1–4) with different methods B3LYP, MP2, and CCSD(T) by using a basis set of 6-31G(d), they observed that the stabilization energies became higher presumably owing to the extensive ionic contribution with increasing the cluster sizes [10].

Sergio F. S. and et al. studied the geometrical parameters for zinc complexes, the results showed that the use of SDD instead of an all-electron basis set has a very limited impact, in terms of accuracy, to determinate the metal-ligand bond-lengths and angles in zinc-complexes [11].

Menbere W. and Hagos W. studied the structural and electronic properties of the small clusters from cadmium telluride, CdnTen and Cd(n−m)ZnmTen for n = 1 − 7 and m = 0 − 3 by using QUANTUM ESPRESSO/ PWSCF package, they found that the structural and electronic properties, and the surface effect changed with cluster size [12].

ZnTe crystallites in zincblende or diamond phase at normal conditions [5, 6]; therefore, in the present work, building blocks called diamondoids are used to build ZnTe nanocrystals. These diamondoids are used successfully for building zincblende or diamond nanocrystals theoretically and experimentally [13, 14]. The structural, electronic and UV-Vis spectrum properties of ZnnTen (n=1, 7, 11, 13) nanocrystals will be investigated theoretically by using Gaussian 09 program and density functional theory DFT and time-dependent density functional theory TD-DFT at the B3LYP level with SDD basis functions [15].

MODELS AND METHOD

Diamondoids and wurtzoids are used successfully to represent the diamond and wurtzite structures at the nano-scale regime, respectively. Diamondoids and wurtzoids nanocrystals are sometimes passivated with other materials such as hydrogen gas to saturate the dangling bonds [13, 14, 16-18]. If not passivated, these unsaturated bonds tend to reconstruct in the surface atom to reduce the surface energy.

The number of cages in their nanostructure determines the diamondoid nomenclatures. As an example, diamondoids of two, three and four cages are called diamantane, triamantane, and tetramantane. For the ZnTe zincblende, only even-numbered cages persist if the number of Zn atoms and Te atoms are kept equal [13]. As an example, ZnTe diamondoids are a diamantane, tetramantane, hexamantane…etc.

Clusters and nanostructures from ZnSe, Zn complexes, CdTe, CdZnTe, and CdSe have been studied theoretically [10-12, 14]. In the present work, ZnTe diamondoids include ZnTe–diamantane (Zn7Te7), ZnTe–tetramantane (Zn11Te11), and ZnTe–hexamantane (Zn13Te13) are used to represent ZnTe nanocrystals. Fig. 1 shows the nanocrystals after geometrically optimized. All calculations in the present work have been done by using Gaussian 09 package, DFT and TD-DFT at the B3LYP level with SDD basis function.

(a)

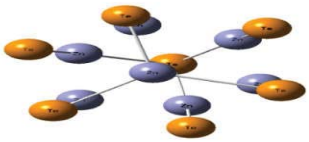

(b)

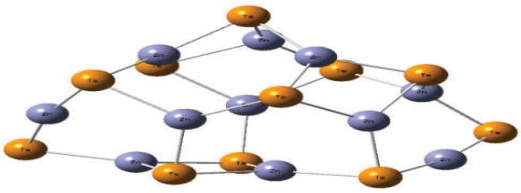

(C)

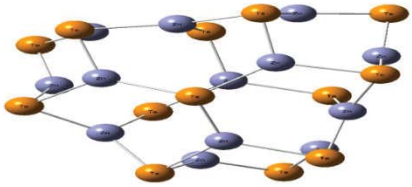

(d)

FIGURE 1. Optimized diamondoids nanostructures (a) diatomic molecule (b) ZnTe, diamantane (Zn_7Te_7) (c) tetramantane ($Zn_{11}Te_{11}$) (d) hexamantane ($Zn_{13}Te_{13}$)

RESULTS AND DISCUSSIONS

Density of bonds

Most atoms in diamondoid nanostructures represent surface atoms. Therefore, the reconstruction in surface atoms deviates many bonds from their experimental length. Fig. 2 shows the distribution of average bond lengths of Zn-Te bonds for diamantane (Zn7Te7), tetramantane (Zn11Te11), and hexamantane (Zn13Te13). All nanostructures have a bond length larger than experimental value due to surface effect is dominants in the nanoscale region; the Surface effect reduces with increasing size of diamondoids due to decrease in the number of dangling bonds for the total number of bonds as shown in Table 1, it is clear from the Table 1, the hexamantane has maximum and minimum values of Zn-Te bond larger than others nanostructures, and the ratio of dangling to total bonds larger than tetramantane due to the configuration of hexamantane structure, therefore the Zn–Te average bond lengths are

2.639 Å in the diamantane, 2.628Å in the tetramantane, and 2.708 Å for hexamantane. It is in good agreement with the experimental value of 2.406 Å [19]. Tetramantane has bond length converge to practical value more than other nanostructures because it has a small ratio of dangling to total bonds.

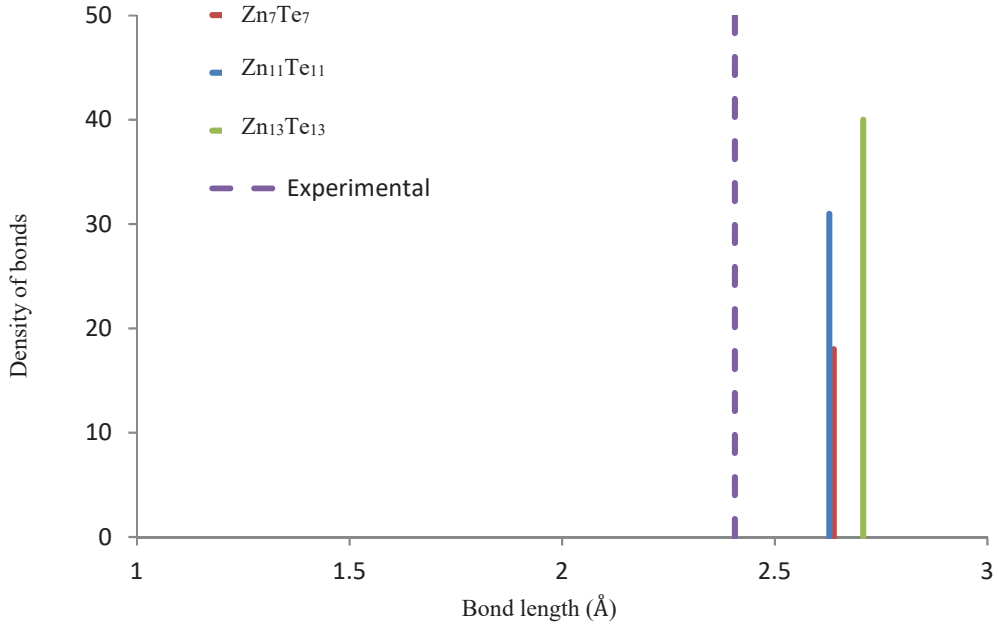

FIGURE 2. Average bond length (Å) for diamantane (Zn_7Te_7), tetramantane ($Zn_{11}Te_{11}$), and hexamantane ($Zn_{13}Te_{13}$).

TABLE 1. Minimum, maximum, and average of Zn-Te bonds, number of dangling bonds and the ratio of dangling to total bonds for the diamondoid nanostructures.

Diamondoids nanostructures	The minimum value of Zn-Te bond (Å)	The maximum value of Zn-Te bond (Å)	Number of dangling bonds	The ratio of dangling to total bonds %	Average of Zn-Te bonds lengths (Å)
Diamantane Zn_7Te_7	2.4607	2.7991	20	52.63	2.639
Tetramantane $Zn_{11}Te_{11}$	2.4506	2.7411	19	35.18	2.628
Hexamantane $Zn_{13}Te_{13}$	2.5273	4.2333	24	37.5	2.708

Binding Energy

Binding energy or separation energy is the minimum energy required to disassemble a nanostructure into isolated atoms or the amount of energy released at the creation of the nanostructures [20]. The binding energy per atom for ZnTe diamondoids nanostructures is calculated by using the relation, $E_{binding} = \frac{(n(Zn+Te)-Zn_nTe_n)}{2n}$, where n is the number of Zn or Te atoms. Figure 3 shows the variation of binding energy per atom for diamondoid nanostructures. It is clear; increasing in diamondoids size causes an increase in the binding energy as shown in Table 2. The tetramantane(Zn11Te11) bonding ability is greater than other diamondoids, possibly because this molecule consists of converging atoms more than other molecules, and the ratio of dangling to total bonds smaller than other molecules, so that it has the smallest average length of Zn-Te bonds. The high value of the binding energy gave tetramantane more stability than other nanostructures.

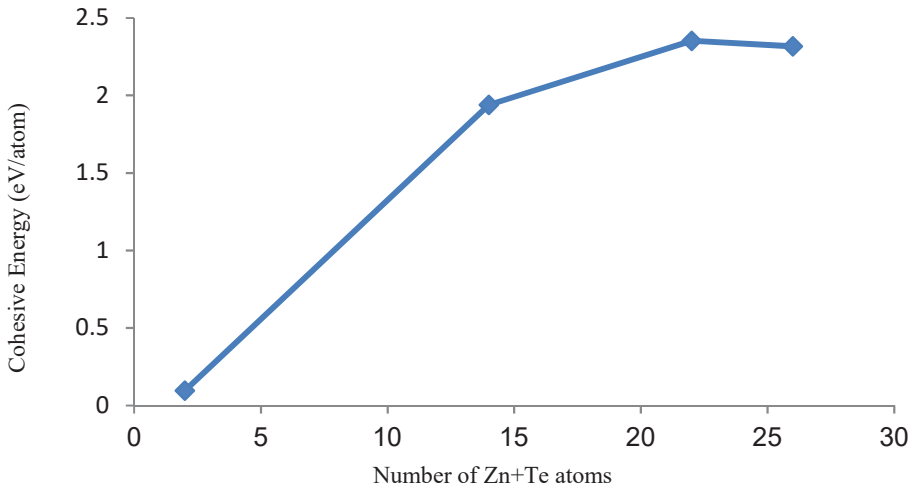

FIGURE 3. The binding energy of Zn+Te diamondoid nanostructures.

Energy Gap

The energy gap reflects the ability for electrons to jump from the high occupied molecular orbital HOMO to lower unoccupied molecular orbital LUMO, so that the physical and chemical activity depends on the value of the energy gap [12]. The energy gap calculated theoretically by the difference between (HOMO-LUMO) energy levels according to the Koopmans theorem [21].

The variation of the energy gap of ZnTe diamondoid nanostructures is shown in Fig. 4. From this figure, it can be noted that the nanostructures tend to touch the bulk experimental bandgap when increasing the size. Nanostructures obey the quantum confinement effect of oncoming to the bulk bandgap with the increase of the size. However, ZnTe diatomic and Zn7Te7 diamantane have a large number of dangling bonds than tetramantane (Zn11Te11) and hexamantane (Zn13Te13), dangling bonds generate energy levels inside the original energy gap. Therefore, the energy gap decreased as shown in Table 2. Increasing in diamondoids size reason decreased in the quantum confinement effect. Hence, energy gap for hexamantane (Zn13Te13) converge to practical value 2.26 eV [22].

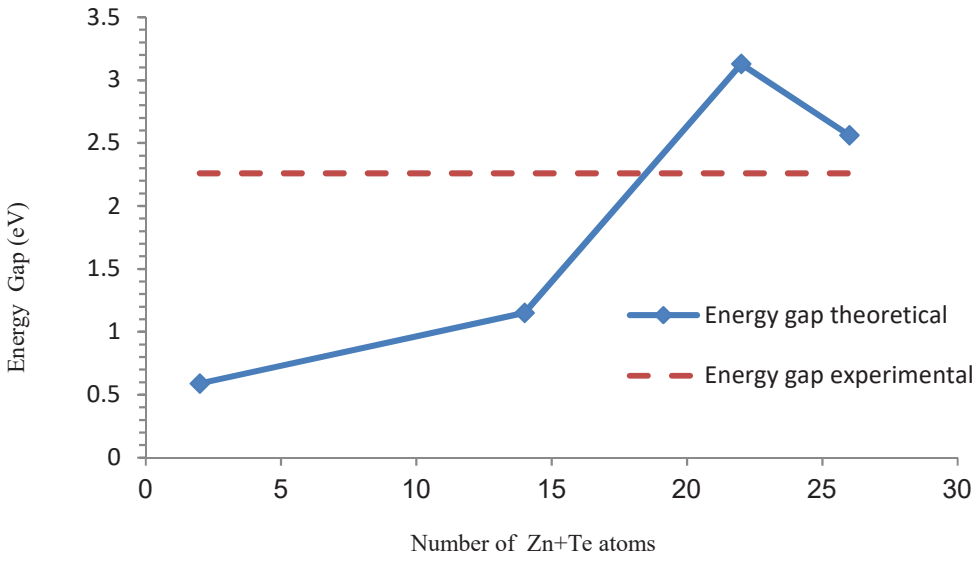

FIGURE 4. The variation of the energy gap of ZnTe diamondoid nanostructures.

TABLE 2. HOMO, LUMO, energy gap, and binding energy for the diamondoid nanostructures.

Diamondoids nanostructures	**HOMO (eV)**	**LUMO (eV)**	**Energy Gap (eV)**	**The experimental value of the energy gap (eV) [22]**	**Binding Energy (eV/atom)**
Diatomic ZnTe	-5.52	-6.11	0.59		0.09
Diamantane Zn_7Te_7	-3.70	-4.85	1.15		1.93
Tetramantane $Zn_{11}Te_{11}$	-2.87	-6.00	3.13	2.26	2.35
Hexamantane $Zn_{13}Te_{13}$	-3.22	-5.78	2.56		2.31

UV-Vis Spectrum

The spectra of UV-Vis for tetramantane (Zn11Te11) and hexamantane (Zn13Te13) are shown in Fig. 5. The optical edge shifts from 268.8 nm for tetramantane (Zn11Te11) to 302.6 nm for hexamantane (Zn13Te13), this shift in excitation energy is due to the increase in the size of the nanostructures. Increasing the optical bandgap at the nanoscale due to the atomic orbitals involved in the overlap region at the nanoscale is much smaller than the bulk. Tetramantane (Zn11Te11) has a maximum peak at 345.6 nm and at 410.4 nm for hexamantane (Zn13Te13) which indications happening redshift. Also, from Fig. 5 shows that the width of the peak increases with increasing the size of diamondoids and extended to near IR region for hexamantane (Zn13Te13). Controlling the optical behavior for ZnTe diamondoid nanostructure by varying the size of the diamondoid leads to varied applications such as in optoelectronic devices, photoelectronic devices, and sensors.

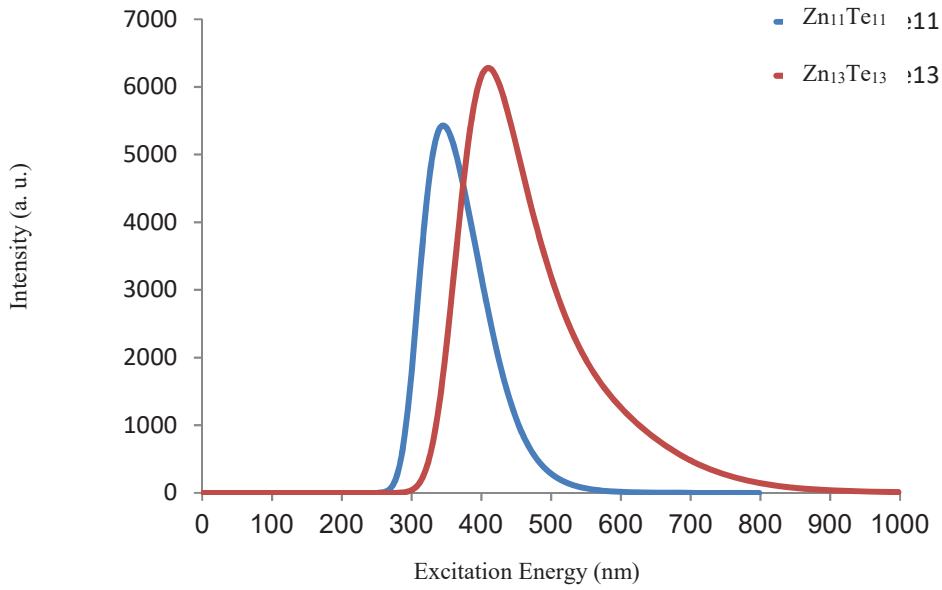

FIGURE 5. UV-Vis spectra of tetramantane ($Zn_{11}Te_{11}$) and hexamantane ($Zn_{13}Te_{13}$).

CONCLUSIONS

Zinc telluride diamondoids nanostructures ZnnTen (n=1, 7, 11, 13) are suggested to represents the zincblende or diamond structures of ZnTe gave results with good agreement with experimental. Tetramantane (Zn11Te11) has a bond length very near to practical value. The stability of tetramantane (Zn11Te11) greater than other diamondoids nanostructures because it has the larger value of the binding energy and smaller ratio of dangling to total bonds than other diamondoids. The energy gap converges to experimental value with different approximately 0.3 eV for hexamantane (Zn13Te13). UV-Vis spectrum for tetramantane (Zn11Te11) has a maximum peak at 345.6 nm while the UV-Vis spectrum for hexamantane (Zn13Te13) at 410.4 nm. Width of the peak increases with the size of diamondoids and expands to near IR region for hexamantane (Zn13Te13). These results refer to the ability to control the properties of the ZnTe nanostructures by variation of the diamondoids size, and these lead to wide applications such as optoelectronic devices, photoelectronic devices, detectors, and sensors.

REFERENCES

1. E. Jimenez-Izal, J. M. Matxain, M. Pirisab, and J. M. Ugaldea, Self-assembling endohedrally doped CdS nanoclusters: new porous solid phases of CdS. Phys. Chem. Chem. Phys. 14, 9676–9682 (2012).
2. T.C.M. Santhosh, K. V. Bangera and G.K. Shivakumar, Synthesis and bandgap tuning in $CdSe_{(1-x)}Te_{(x)}$ thin films for solar cell applications. Sol. Energy 153, 343–347 (2017).
3. S. N.Saravanamoorthy, A. J. Peter and C. W.Lee, Optical peak gain in a PbSe/CdSe core-shell quantum dot in the presence of magnetic field for mid-infrared laser applications. Chem. Phys. 483–484 (2017).
4. H. H. Abed, H. M. Abduljalil, and M. A. Abdulsattar, Structural, Optical and Humidity Sensitivity for CdSe Nanocrystalline Thin films. J. Adv. Pharm. Edu. Res. 8, 4. 52-31 (2018).
5. N. Srimathy and A. Ruban Kumar, Deposition and Characterisation of Zinc Telluride as a Back Surface Field Layer in Photovoltaic Applications, Mechanics, Materials Science & Engineering, (2017).
6. M. Jayachandran, P. Ponsurya, Abbas Shahul Hameed BH., and A. Ayeshamariam, RBS Analysis of Zinc Telluride Thin Films by Electron Beam Evaporation Technique, Fluid Mech. 4, (2017).
7. D. C. Sharma, S. Srivastava, Y.K. Vijay, and Y.K. Sharma, Effect of Mn-Doping on Optical Properties of ZnTe Thin Films. International Journal of Recent Research and Review,4,(2012).
8. S. A. Maki and H. K. Hassun, The Structural and Optical Properties of Zinc Telluride Thin Films by Vacuum Thermal Evaporation Technique, Ibn Al-Haitham J. for Pure & Appl. Sci. 29,(2016).

9. Q. Zhang, J. Zhang, M. I. B. Utama, B. Peng, M. de la Mata, J. Arbiol, and Qihua Xiong, Exciton-phonon coupling in individual ZnTe nanorods studied by resonant Raman spectroscopy, Physical L Review B 85, 085418 (2012).
10. B. H. Boo, H. Cho, and D. E. Kang, Ab initio and DFT investigation of structures and energies of low-lying isomers of Zn_xSe_x (x = 1–4) clusters. Journal of Molecular Structure: Theochem 806, 77–83 (2007).
11. S. F. Sousa, E. S. Carvalho, D. M. Ferreira, I. S. Tavares, P. A. Fernandes, M. J. Ramos, J. A. N. F. Gomes, Comparative Analysis of the Performance of Commonly Available Density Functionals in the Determination of Geometrical Parameters for Zinc Complexes, J Comput Chem 30, 2752–2763 (2009).
12. M. Weldetsadik1 and H. Woldeghebriel, A DFT Study on the Structural and Electronic Properties of Cadmium Telluride (Cd_nTe_n) and Cadmium Zinc Telluride ($Cd_{(n-m)}Zn_mTe_n$) Clusters, Momona Ethiopian Journal of Science (MEJS), 7,105-124 (2015).
13. M. A. Abdulsattar and I. S. Mohammed, Diamondoids and large unit cell method as building blocks of InAs nanocrystals: A density functional theory study, Computational Materials Science, 91 11–14 (2014).
14. M. A. Abdulsattar, H. M. Abduljalil, and H. H. Abed, Formation energies of CdSe wurtzoid and diamondoid clusters formed from Cd and Se atomic clusters. Calphad. 64, 37–42 (2019).
15. Gaussian 09, Revision E.01, M. J. Frisch, G. W. Trucks, H. B. Schlegel, G. E. Scuseria, M. A. Robb, J. R. Cheeseman, G. Scalmani, V. Barone, B. Mennucci, G. A. Petersson, H. Nakatsuji, M. Caricato, X. Li, H. P. Hratchian, A. F. Izmaylov, J. Bloino, G. Zheng, J. L. Sonnenberg, M. Hada, M. Ehara, K. Toyota, R. Fukuda, J. Hasegawa, M. Ishida, T. Nakajima, Y. Honda, O. Kitao, H. Nakai, T. Vreven, J. A. Montgomery, Jr, J. E. Peralta, F. Ogliaro, M. Bearpark, J. J. Heyd, E. Brothers, K. N. Kudin, V. N. Staroverov, R. Kobayashi, J. Normand, K. Raghavachari, A. Rendell, J. C. Burant, S. S. Iyengar, J. Tomasi, M. Cossi, N. Rega, J. M. Millam, M. Klene, J. E. Knox, J. B. Cross, V. Bakken, C. Adamo, J. Jaramillo, R. Gomperts, R. E. Stratmann, O. Yazyev, A. J. Austin, R. Cammi, C. Pomelli, J. W. Ochterski, R. L. Martin, K. Morokuma, V. G. Zakrzewski, G. A. Voth, P. Salvador, J. J. Dannenberg, S. Dapprich, A. D. Daniels, O. Farkas, J. B. Foresman, J. V. Ortiz, J. Cioslowski, and D. J. Fox, Gaussian, Inc., Wallingford CT, (2009).
16. M. A. Abdulsattar, GaN wurtzite nanocrystals approached using wurtzoids structures and their use as a hydrogen sensor: A DFT study. Superlattices Microstruct. 93, 163-170 (2016).
17. M. A. Abdulsattar, Chlorine gas reaction with ZnO wurtzoid nanocrystals as a function of temperature: a DFT study. J. Mol. Model., 23, 125 (2017).
18. M. A. Abdulsattar, H. M. Abduljalil, and H. H. Abed, Structure, Stability and Vibrational Properties of CdSe Wurtzite Molecules and Nanocrystals: A DFT Study. Karbala International Journal of Modern Science. 5, 119-125 (2019).
19. H. Khlyap, From Semiclassacial Semiconductors to Noval Spintronic Devices, Bentham Science Publishers (2013).
20. H. W. Hugosson, A Theoretical Treatise on the Electronic Structure of Designer Hard Materials, Literature publishes, Wilhelm, (2001).
21. M. Weinert, E. Wimmer, and A. J. Freeman, Materials Design Application Note, Phys. Rev., 26, 1-6, (2008).
22. V. Kumar, V. Kumar and D. K. Dwivedi, Growth and characterization of zinc telluride thin films for photovoltaic applications, Phys. Scr. 86 (2012).